

### **3.0 Turbulent Boundary Layer and Shear Layer Theory**

A brief review of simple theory for turbulent boundary layers and shear layers will aid in the understanding of the development and calibration of turbulence models. Most of these relationships are based on empirical correlations of the shape of the velocity profile across the boundary layer or shear layer. This shape can be used in conjunction with the Navier-Stokes equations to back out relationships for the turbulent stresses or the eddy viscosity.

#### **3.1 Boundary Layer Theory**

Turbulent boundary layers are usually described in terms of several nondimensional parameters. The boundary layer thickness,  $\delta$ , is the distance from the wall at which viscous effects become negligible and represents the edge of the boundary layer. Two integral parameters across the velocity profile are the displacement thickness  $\delta^*$  and the momentum thickness  $\theta$ .

$$\delta^* = \int_0^\infty \left(1 - \frac{\rho u}{\rho_e u_e}\right) dy \quad (3.1)$$

$$\theta = \int_0^\infty \frac{\rho u}{\rho_e u_e} \left(1 - \frac{u}{u_e}\right) dy \quad (3.2)$$

The integration is performed normal to the wall and the subscript  $e$  is used to denote the edge of the boundary layer at  $y=\delta$ . The displacement thickness is a measure of the increased thickness of a body due to the velocity defect of the boundary layer. The momentum thickness is the distance that, when multiplied by the square of the free-stream velocity, equals the integral of the momentum defect across the boundary layer.

If a simple power law velocity profile as shown in Eq. 3.3 is assumed and the flow is incompressible, the relationships in Eqs. 3.4-3.7 can be obtained from approximations of the Navier-Stokes equations.

$$\frac{u}{u_e} = \left(\frac{y}{\delta}\right)^{1/7} \quad (3.3)$$

$$\frac{\delta}{x} = \frac{0.371}{\text{Re}_x^{1/5}} \quad (3.4)$$

$$\frac{\delta^*}{x} = \frac{0.046}{\text{Re}_x^{1/5}} \quad (3.5)$$

$$\frac{\theta}{x} = \frac{0.036}{\text{Re}_x^{1/5}} \quad (3.6)$$

$$C_f = \frac{\tau_w}{\frac{1}{2} \rho_e u_e^2} = \frac{0.0577}{\text{Re}_x^{1/5}} \quad (3.7)$$

$C_f$  is called the skin friction. The distance from the leading edge in the streamwise direction is given by  $x$ . Both the boundary layer growth rate and the skin friction decrease as the Reynolds number increases.

Reynolds analogy can be used to develop a relationship for heat transfer. Reynolds analogy says that the ratio of the shear stress to the heat transfer is a constant near the wall. Thus the Nusselt number can be defined as

$$\text{Nu}_x = \frac{hx}{k} = \frac{C_f}{2} \text{Re}_x \text{Pr} \quad (3.8)$$

Here  $h$  is the heat transfer coefficient,  $k$  is the thermal conductivity, and  $\text{Pr}$  is the Prandtl number. This relationship is independent of the equation used to determine skin friction.

The power law relationship is not extremely accurate, but is useful for developing some useful turbulent boundary layer relationships. A more accurate relationship for skin friction for adiabatic incompressible flow on a flat plate is given by White and Christoph<sup>1</sup>

$$C_f = \frac{0.42}{\ln^2(0.056 \text{Re}_x)} \quad (3.9)$$

This relationship is only applicable in the turbulent region of a boundary layer, and does not apply in the laminar or transitional regions of the boundary layer. The skin friction is affected by a number of parameters, including pressure gradient, surface roughness, compressibility, and surface heat transfer. Adverse pressure gradients cause the skin friction to be reduced as the boundary layer is pushed toward separation. Boundary layer separation occurs when the skin friction becomes negative. High values of skin friction are an indication of a very stable (i.e. difficult to separate) boundary layer. Unfortunately high values of skin friction also equate to high values of viscous drag. The effect of both compressibility and heat transfer on the flat plate turbulent skin friction are shown in Fig. 3.1. Both a hot wall and compressibility tend to reduce the skin friction over the incompressible adiabatic value.

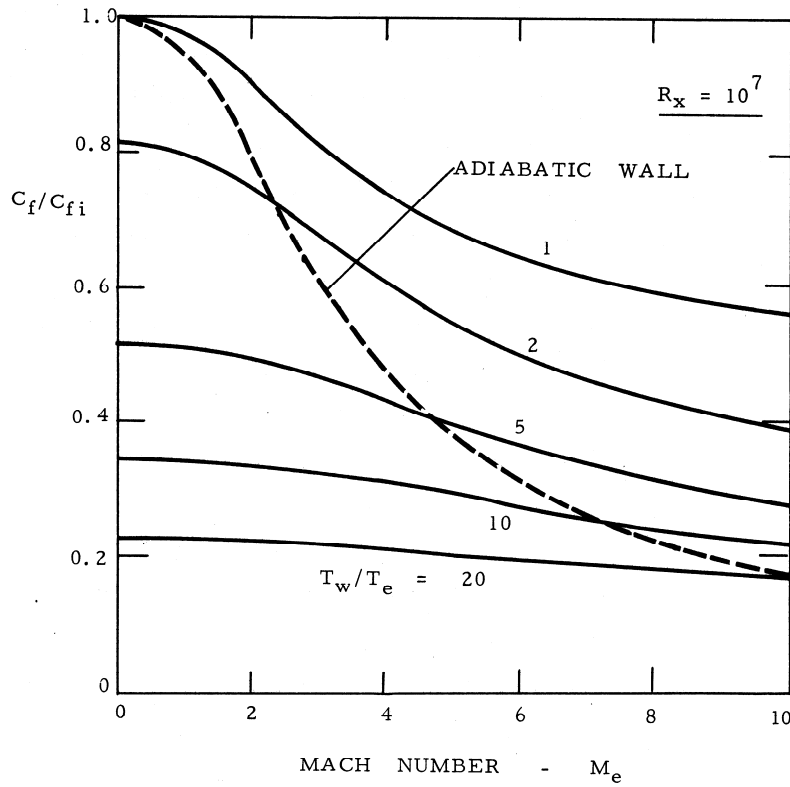


Figure 3.1 Effect of compressibility and heat transfer on the skin friction on a flat plate.

As mentioned above, the power law relationship in Eq. 3.3 is not very accurate. Better approximations of the velocity profile shape are generally written in terms of the parameters  $u^+$  and  $y^+$  defined as

$$u^+ = \frac{u}{u_\tau} \quad (3.10)$$

$$y^+ = \frac{\rho_w u_\tau y}{\mu_w} \quad (3.11)$$

and  $u_\tau$  is the friction velocity

$$u_\tau = \sqrt{\frac{\tau_w}{\rho_w}} \quad (3.12)$$

The subscript  $w$  denotes the value at the wall and  $\tau_w$  is the wall shear stress defined by

$$\tau_w = \mu \left. \frac{\partial u}{\partial y} \right|_w \quad (3.13)$$

The boundary layer velocity profile can be divided into four regions. The incompressible velocity profile in each of the subregions regions of the inner region shown in Fig. 3.2 is given by

$$\text{Laminar sublayer} \quad 0 < y^+ < 5 \quad u^+ = y^+ \quad (3.14)$$

$$\text{Buffer layer} \quad 5 < y^+ < 30 \quad u^+ = 5 \ln y^+ - 3.05 \quad (3.15)$$

$$\text{Log layer} \quad 30 < y^+ < 1000 \quad u^+ = \frac{1}{\kappa} \ln y^+ + B \quad (3.16)$$

The values of  $\kappa$ , the von Karmen constant, and  $B$  are often debated, but are generally accepted to be 0.4 and 5.5 respectively. The log layer is also called the law of the wall.

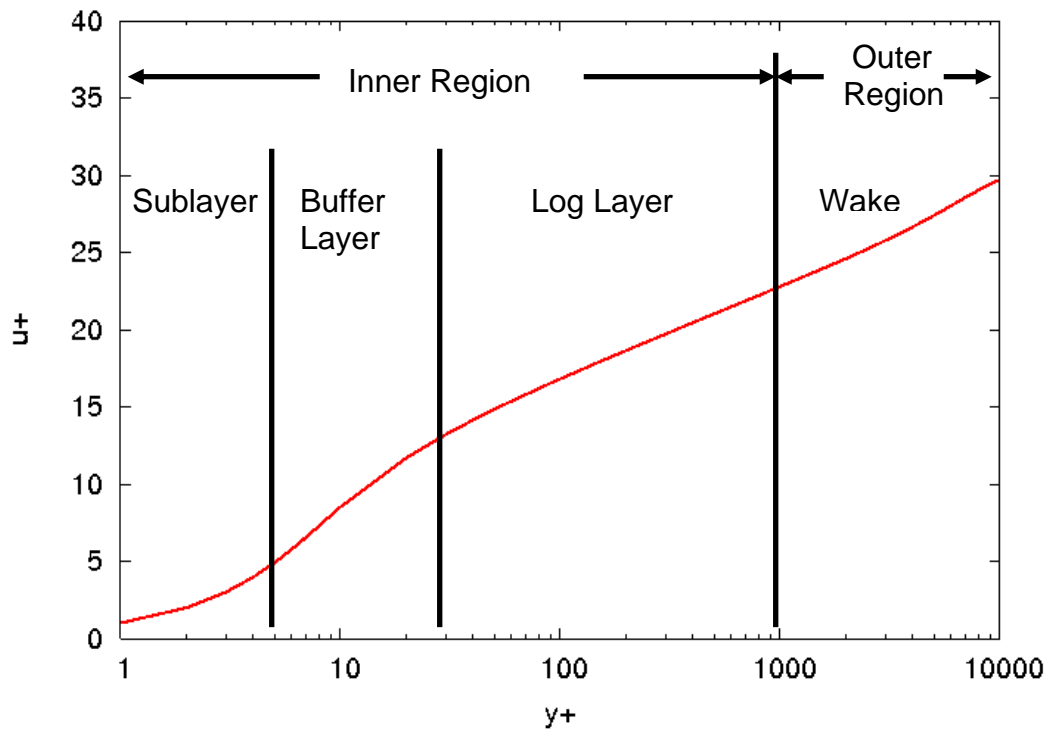


Figure 3.2 Boundary layer regions.

The  $y^+$  value where the profile transitions from the inner to the outer profile varies with the Reynolds number and the pressure gradient. The outer region is much more sensitive to pressure gradient. Clauser's<sup>2</sup> equilibrium parameter  $\beta$  is often used to characterize the pressure gradient.

$$\beta = \frac{\delta^*}{\tau_w} \frac{\partial p_e}{\partial x} \quad (3.17)$$

Coles<sup>3</sup> introduced the wake function  $W$  given by

$$W\left(\frac{y}{\delta}\right) = 2 \sin^2\left(\frac{\pi}{2} \frac{y}{\delta}\right) \quad (3.18)$$

The velocity profile in the outer region is given by

$$u^+ = \frac{1}{\kappa} \ln y^+ + B + \frac{\Pi}{\kappa} W\left(\frac{y}{\delta}\right) \quad (3.19)$$

where  $\Pi$  is given by

$$\Pi = 0.8(\beta + 0.5)^{0.75} \quad (3.20)$$

Spalding<sup>4</sup> proposed a composite form for the incompressible velocity profile given by

$$y^+ = u^+ + e^{-\kappa B} e^{-\Pi W} \left[ e^{\kappa u^+} - 1 - \kappa u^+ - \frac{(\kappa u^+)^2}{2} - \frac{(\kappa u^+)^3}{6} \right] \quad (3.21)$$

White and Christoph<sup>1</sup> give a law of the wall velocity profile that includes the effects of compressibility, heat transfer, and pressure gradient.

$$\sin^{-1}\left(\frac{2\Gamma u^+ - \Theta}{Q}\right) = \sin^{-1}\left(\frac{2\Gamma u_0^+ - \Theta}{Q}\right) + \frac{\Gamma^{1/2}}{\kappa} \left[ 2(\phi - \phi_0) + \ln\left(\frac{\phi - 1}{\phi + 1} \frac{\phi_0 + 1}{\phi_0 - 1}\right) \right] \quad (3.22)$$

Where  $Q = (\Theta^2 + 4\Gamma)^{1/2}$  and  $\phi = (1 + \alpha y^+)^{1/2}$ . The values of  $y_0^+$  and  $u_0^+$  are taken as 6 and 10 respectively. The parameters  $\Theta$ ,  $\Gamma$ , and  $\alpha$  represent the effects of heat transfer, compressibility, and pressure gradient respectively.

$$\Theta = \frac{q_w \mu_w}{T_w k_w \rho_w u_\tau} \quad (3.23)$$

$$\Gamma = \frac{r u_\tau^2}{2c_p T_w} \quad (3.24)$$

$$\alpha = \frac{\mu_w}{\rho_w \tau_w u_\tau} \frac{\partial p_e}{\partial x} \quad (3.25)$$

Here  $q_w$  is the wall heat transfer ( $k_w \frac{\partial T}{\partial y}|_w$ ),  $\mu_w$  is the wall viscosity,  $T_w$  is the wall temperature,  $\rho_w$  is the wall density,  $r$  is the recovery factor (normally taken as the Prandtl number to the one third power),  $k_w$  is the wall thermal conductivity, and  $c_p$  is the specific heat at constant pressure.

It is not obvious what effect each of the parameters defined in Eqs. 3.23-25 has on the velocity profile. Fig. 3.3 shows the effect of an adverse pressure gradient and compressibility has on the velocity profile.

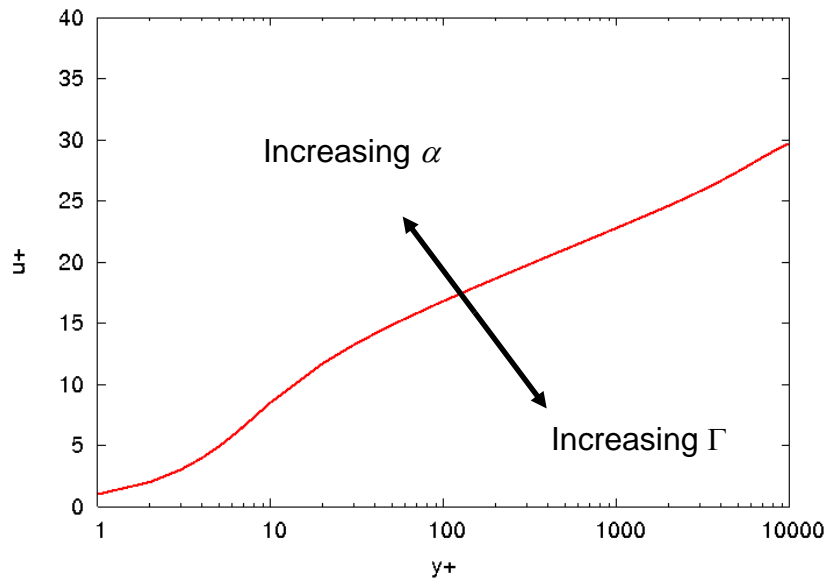


Figure 3.3 Effect of adverse pressure gradient and compressibility on boundary layer profile shape.

The boundary layer thickens and the skin friction decreases as the pressure gradient is increased. Compressibility also causes the skin friction to decrease. Heat transfer effects are shown in Fig. 3.4.

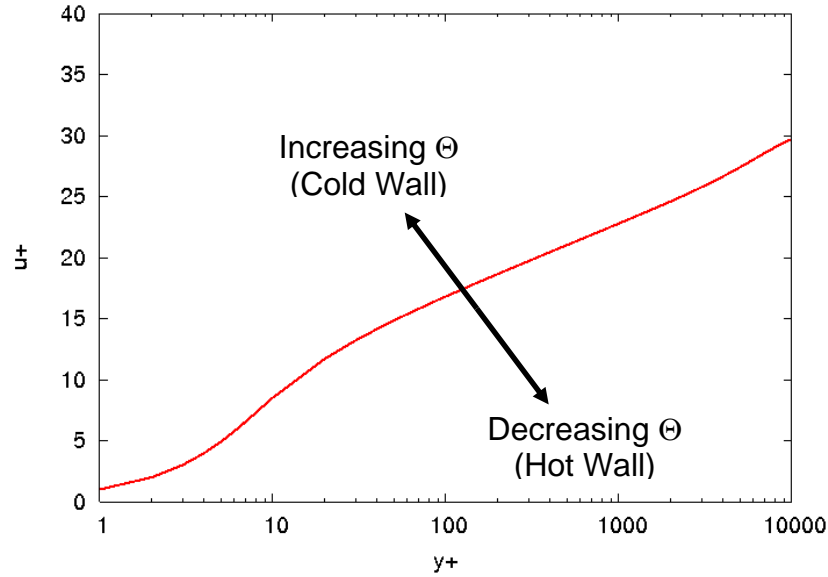


Figure 3.4 Effect of wall heat transfer on boundary layer profile shape.

A cold wall (wall temperature less than the adiabatic wall temperature) creates a thinner boundary layer and increases the skin friction. A hot wall (wall temperature greater than the adiabatic wall temperature) thickens the boundary layer and decreases the skin friction.

The temperature distribution within the inner part of the boundary layer boundary layer is given by the Crocco-Busemann equation

$$T = T_w \left( 1 + \Theta u^+ - \Gamma (u^+)^2 \right) \quad (3.26)$$

where  $\Theta$  is defined in Eq. 3.23 and  $\Gamma$  is defined in Eq. 3.24. For adiabatic wall cases,  $\beta = 0$  and the Crocco-Busemann equation reduces to

$$T = T_w \left( 1 + \frac{(\gamma - 1)r}{2} u^2 \right) \quad (3.27)$$

The pressure is assumed to be constant in the normal direction from the wall in the inner part of the boundary layer. Density distributions can be defined based on the temperature distribution and the equation of state.

### **3.2 Shear Layer Theory**

A free shear layer is always initiated from a surface of some kind. The boundary layer profile remains for a short period. If no external pressure gradient is present, the shear layer will eventually become self-similar. A self-similar profile is one in which the profile shape remains unchanged as you move downstream if

the profile is defined in terms of similarity variables. Chapman and Korst<sup>5</sup> suggested the similarity variable for two-dimensional shear layers

$$\eta = \frac{\sigma y}{x} \quad (3.28)$$

where  $x$  is the downstream distance from the origin of the shear layer,  $y$  is the normal distance across the shear layer ( $y=0$  denotes the center of the shear layer), and  $\sigma$  is the shear layer spread rate parameter. Brown and Roshko<sup>6</sup> suggested using

$$y^* = \frac{y - y_{0.5}}{\delta_\omega} \quad (3.29)$$

where the vorticity thickness  $\delta_\omega$  is defined as

$$\delta_\omega = \frac{U_1 - U_2}{\left(\frac{\partial u}{\partial y}\right)_{\max}} \quad (3.29)$$

Here  $U_1$  is the velocity at the high speed edge of the shear layer and  $U_2$  is the velocity at the low speed edge of the shear layer. Chapman and Korst<sup>5</sup> suggested that the velocity profile was given by

$$u^* = \frac{u}{U_1 - U_2} = 0.5[1 + \operatorname{erf}(\eta)] \quad (3.30)$$

where  $\operatorname{erf}$  is the error function. This profile shape is valid for both laminar and turbulent shear layers. Samimy and Elliot<sup>7</sup> obtained Laser Doppler Velocimeter (LDV) data on a shear layer. Measurements were made at several downstream locations between the trailing edge of the splitter plate and a station 210 mm downstream of the splitter plate. The flow parameters are given in Table 3.1. Eq. 3.30 is plotted with data in Fig. 3.5.

$T_0$ , K	$P_{01}$ , kPa	$M_1$	$M_2$	$M_c$	$U_1$ , m/sec	$U_2/U_1$	$\rho_2/\rho_1$	$\delta_1$ , mm
291.0	314.0	1.80	0.51	0.52	479.5	0.355	0.638	8.0

Table 3.1 Flow parameters for the spatial mixing-layer case



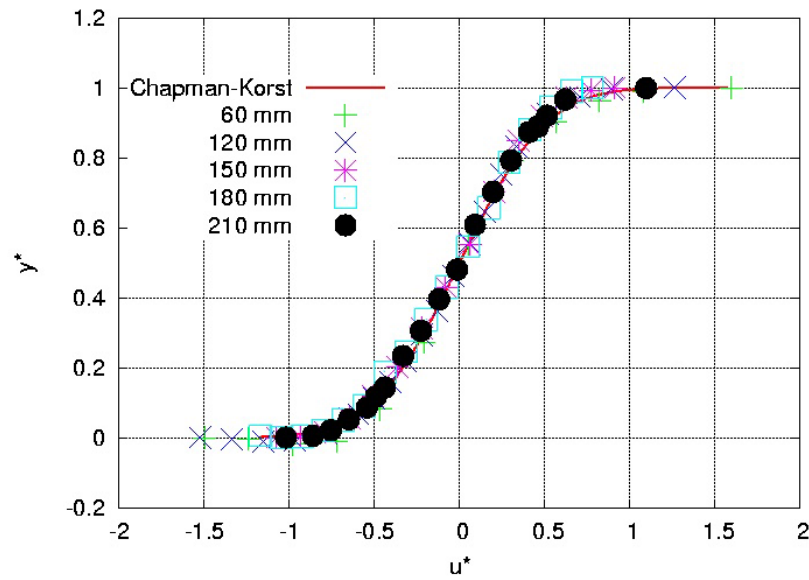


Figure 3.5 Shear layer velocity profile.

The shear layer thickness is given by

$$b = \frac{x}{\sigma} \quad (3.31)$$

The shear layer spread parameter ( $\sigma$ ) is affected by compressibility. The accepted value for subsonic flow issuing into quiescent air is  $\sigma \approx 11$ . This value will increase as compressibility effects become greater, and will cause the shear layer to become thinner. Experimental values<sup>8</sup> for  $\sigma$  for two-dimensional jets issuing into quiescent air are shown in Fig. 3.6.

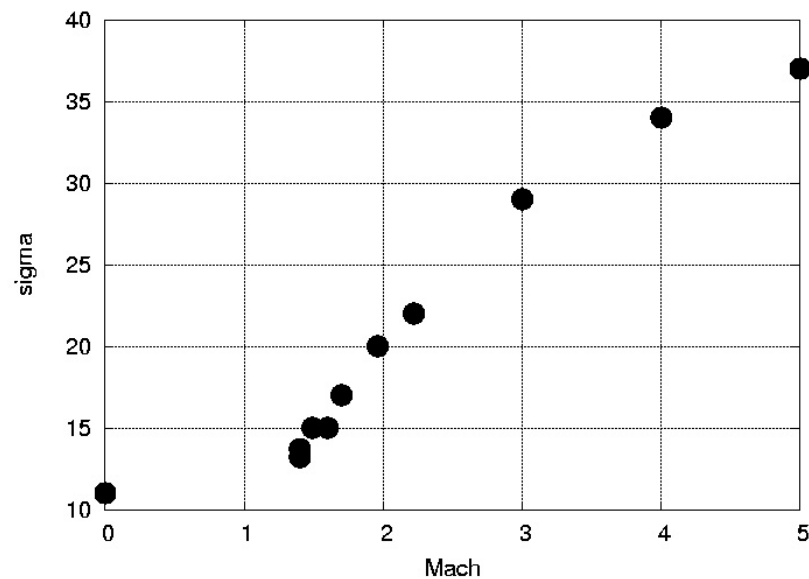


Figure 3.6 Shear layer spread parameter for jet issuing into quiescent air.

Subsonic spread parameter experimental results<sup>8</sup> as a function of velocity ratio for are shown in Fig. 3.7.

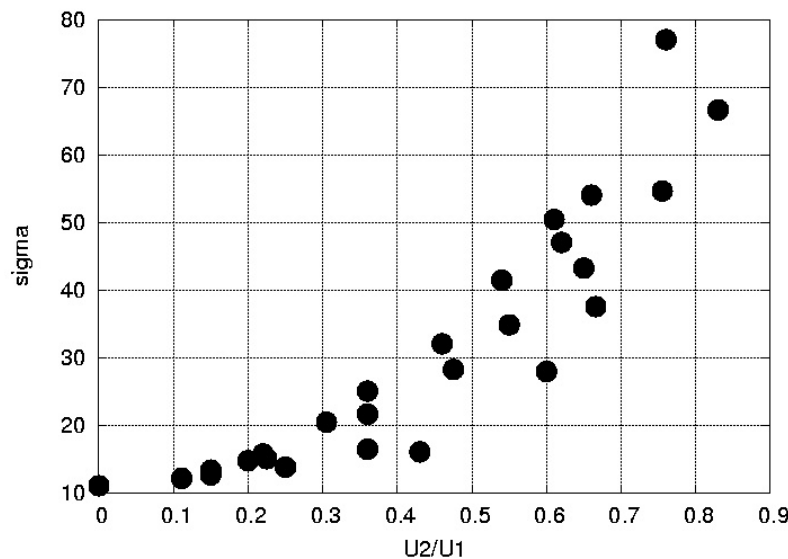


Figure 3.7 Shear layer spread parameter for subsonic jets.

### **Chapter 3 References:**

1. White, F. M. and Christoph, G. H., "A Simple New Analysis of Compressible Turbulent Two-Dimensional Skin Friction Under Arbitrary Conditions," AFFDL-TR-70-133, Feb. 1971.
2. Clauser, F. J., "Turbulent Boundary Layers in Adverse Pressure Gradients," *Journal of the Aeronautical Sciences*, Vol. 21, 1954, pp. 91-108.
3. Coles, D. "The Law of the Wake in the Turbulent Boundary Layer," *Journal of Fluid Mechanics*, Vol. 1, Part 2, July 1956, pp. 191-226.
4. Spalding, D. B., "A Single Formula for the Law of the Wall," *Journal of Applied Mechanics*, Vol. 28, No. 3, 1961, pp. 444-458.
5. Chapman, A. and Korst, H., "Free Jet Boundary with Consideration of Initial Boundary Layer," *Proceedings of the Second U. S. National Congress of Applied Mechanics*, The American Society of Mechanical Engineers, New York, 1954, pp. 723-731.
6. Brown. G. and Roshko, A., "On Density Effects and Large Structure in Turbulent Mixing Layers," *Journal of Fluid Mechanics*, Vol. 64, No. 4, 1974, pp. 775-816.
7. Samimy, M. and Elliot, G., "Effects of Compressibility on the Characteristics of Free Shear Layers," *AIAA Journal*, Vol. 28, No. 3, 1990, pp. 439-445.
8. Birch, S. and Eggers, J., "A Critical Review of Experimental Data for Developed Free Turbulent Shear Layers," in *Free Turbulent Shear Flows*, NASA-SP-321, 1972, pp. 11-37.